

Glucagon Receptor Signaling Is Essential for Control of Murine Hepatocyte Survival

ELAINE M. SINCLAIR,* BERNARDO YUSTA,* CATHERINE STREUTKER,† LAURIE L. BAGGIO,* JACQUELINE KOEHLER,* MAUREEN J. CHARRON,§ and DANIEL J. DRUCKER*

*Department of Medicine, Mt. Sinai Hospital, Samuel Lunenfeld Research Institute, and the †Department of Pathology, St Michael's Hospital, University of Toronto, Toronto, Ontario, Canada; and the §Department of Biochemistry, Albert Einstein College of Medicine, Bronx, New York

Background & Aims: Glucagon action in the liver is essential for control of glucose homeostasis and the counterregulatory response to hypoglycemia. Because receptors for the related peptides glucagon-like peptide-1 and glucagon-like peptide-2 regulate β -cell and enterocyte apoptosis, respectively, we examined whether glucagon receptor (Gcgr) signaling modulates hepatocyte survival. **Methods:** The importance of the Gcgr for hepatocyte cell survival was examined using Gcgr^{+/+} and Gcgr^{-/-} mice in vivo, and murine hepatocyte cultures in vitro. **Results:** Gcgr^{-/-} mice showed enhanced susceptibility to experimental liver injury induced by either Fas Ligand activation or a methionine- and choline-deficient diet. Restoration of hepatic Gcgr expression in Gcgr^{-/-} mice attenuated the development of hepatocellular injury. Furthermore, exogenous glucagon administration reduced Jo2-induced apoptosis in wild-type mice and decreased caspase activation in fibroblasts expressing a heterologous Gcgr and in primary murine hepatocyte cultures. The anti-apoptotic actions of glucagon were independent of protein kinase A, phosphatidylinositol-3K, and mitogen-activated protein kinase, and were mimicked by the exchange protein directly activated by the cyclic AMP agonist 8-(4-chlorophenylthio)-2'-O-methyladenosine-3', 5'-cyclic monophosphate-cAMP. **Conclusions:** These findings extend the essential actions of the Gcgr beyond the metabolic control of glucose homeostasis to encompass the regulation of hepatocyte survival.

Glucagon is a 29 amino acid proglucagon-derived peptide released from pancreatic α -cells that regulates blood glucose via stimulation of hepatic gluconeogenesis and glycogenolysis.¹ Glucagon also inhibits glycogen synthesis and glycolysis and is the primary counter-regulatory hormone to insulin. Loss of the α -cell glucagon response to hypoglycemia and dysregulation of glucagon secretion contribute to the pathophysiology of diabetes mellitus. Because inappropriately increased levels of plasma glucagon increase hepatic glucose production leading to hyperglycemia, there is considerable interest in determining whether diminution

of glucagon action may be useful for the treatment of type 2 diabetes.¹

The biological importance of the glucagon receptor (Gcgr) has been analyzed via characterization of Gcgr^{-/-} mice that show modest fasting hypoglycemia, and improved glucose tolerance.² Gcgr^{-/-} mice also show reduced adiposity, decreased circulating triglycerides, improved insulin sensitivity, and increased circulating levels of glucagon-like peptide-1 (GLP-1).^{2,3} Moreover, after high-fat feeding, Gcgr^{-/-} mice show decreased body weight and food intake, reduced plasma glucose levels, and improved glucose tolerance.⁴

The diabetes-resistant phenotype of Gcgr^{-/-} mice, taken together with observations that the glucose-lowering actions of amylin, GLP-1 receptor agonists, and dipeptidyl peptidase-4 inhibitors are attributable in part to inhibition of inappropriate glucagon secretion,⁵ has rekindled interest in attenuation of glucagon action for the treatment of diabetes. Indeed, reduction of liver Gcgr expression using antisense oligonucleotides leads to reduced hepatic glucose production and amelioration of experimental diabetes^{6,7} and small-molecule Gcgr antagonists attenuate glucagon action in human subjects.

Although glucagon, GLP-1, and GLP-2 exert distinct biological actions through separate G-protein-coupled receptors,⁸ these peptides also share overlapping mechanisms of action. GLP-1 and GLP-2 regulate glucose homeostasis and nutrient absorption, respectively, and both peptides enhance cell survival via cAMP-dependent pathways. Intriguingly, glucagon also acts as a growth and/or survival factor for cultured hepatocytes in vitro.^{9,10} To determine the importance of Gcgr action for hepatocyte survival, we studied the consequences of enhanced or

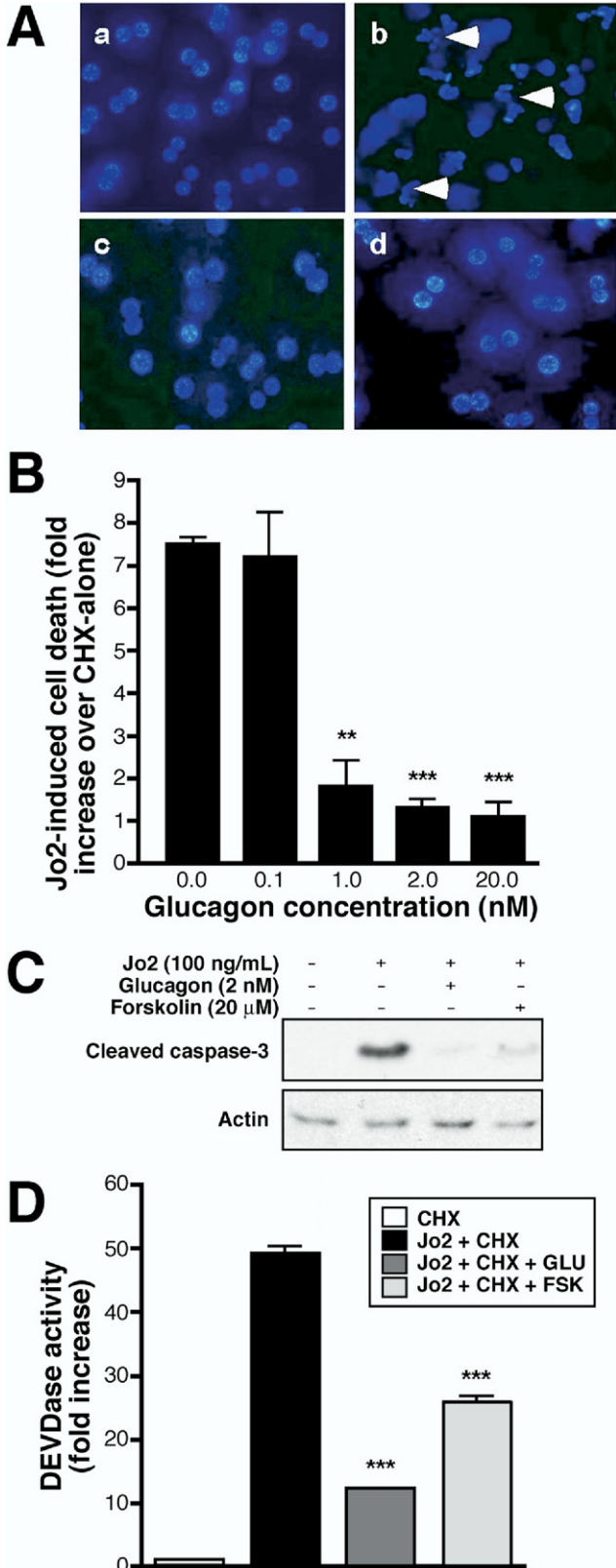
Abbreviations used in this paper: BHK, baby hamster kidney; CHX, cycloheximide; DISC, death-inducing signaling complex; Epac, exchange protein directly activated by cyclic AMP; Gcgr, glucagon receptor; GLP-1, glucagon-like peptide-1; GLP-2, glucagon-like peptide-2; PKA, protein kinase A; rGcgr, rat glucagon receptor.

© 2008 by the AGA Institute

0016-5085/08/\$34.00

doi:10.1053/j.gastro.2008.07.075

disrupted Gcgr signaling in murine hepatocytes. We show here that Gcgr signaling is essential for hepatocyte survival via regulation of cAMP-dependent pathways linked to attenuation of caspase activity.



Materials and Methods

Materials

Tissue culture reagents were from Invitrogen (Burlington, Ontario, Canada) and chemicals were from Sigma-Aldrich (St Louis, MO). Human glucagon was purchased from California Peptides (Napa, CA). H-89, LY294002, and U0126 were from Calbiochem (Gibbstown, NJ). Primary tissue culture plates were from BD Biosciences (San Jose, CA). Anti-Fas antibody (Jo2) was from BD Pharmingen (San Jose, CA) and the exchange protein directly activated by cyclic AMP (Epac) agonist 8-pCPT-Me-cAMP was from Biolog Life Sciences Institute (San Diego, CA).

Baby Hamster Kidney Cell Culture

Baby hamster kidney (BHK):rat Gcgr (rGcgr) cells¹¹ were cultured in 4.5 g/L glucose and Dulbecco's modified Eagle medium, supplemented with 10% fetal bovine serum containing G418 (0.8 mg/mL). When 70%–80% confluence was reached, cells were serum-deprived for 16–24 hours before induction of apoptosis with cycloheximide.

Cell Viability and Proliferation Assays

Cell viability was assessed by measuring bioreduction of a MTS (3-(4,5-dimethylthiazol-2-yl)-5-(3-carboxymethoxyphenyl)-2-(4-sulfophenyl)-2H-tetrazolium) tetrazolium salt at 490 nm using the Cell Titer 96 aqueous assay (Promega, San Luis Obispo, CA). Cell proliferation of BHK:rGcgr cells was determined using a bromodeoxyuridine proliferation enzyme-linked immunosorbent assay kit (Roche, Indianapolis, IN).

cAMP Measurement

Measurement of total cAMP was performed using a radioimmunoassay kit from Biomedical Technologies, Inc (Stoughton, MA).

Figure 1. (A) Glucagon and forskolin protect primary mouse hepatocytes from apoptosis. Assessment of nuclear morphology in 4'-6-diamidino-2-phenylindole-stained mouse hepatocytes after treatment for 4–5 hours with 10 μmol/L CHX (a) or with 10 μmol/L CHX plus 100 ng/mL Jo2 in the absence (b) or presence of 2 nmol/L glucagon (c) or 20 μmol/L forskolin (d). Arrowheads in b indicate cells undergoing apoptosis. Magnification in a–d, 400×. (B) Mouse hepatocytes were exposed to 10 μmol/L CHX plus 100 ng/mL Jo2 in the absence or presence of glucagon. After 4–5 hours apoptosis was quantified using the Cell Death enzyme-linked immunosorbent assay kit. Data are expressed as fold-increase relative to CHX-alone-treated cultures and are mean ± SD from 2 independent experiments. **P < .01, ***P < .001, CHX and Jo2 plus glucagon vs CHX plus Jo2 alone. Cell extracts from primary mouse hepatocytes treated with CHX alone or CHX plus Jo2 with or without glucagon or forskolin for 4–5 hours were analyzed by Western blotting for (C) cleaved caspase-3 or for (D) DEVD hydrolase activity. Results are representative of 4 independent experiments. DEVDase activity data are mean ± SD and represent 3 independent experiments each performed in duplicate. ***P < .001, CHX plus Jo2 and glucagon or forskolin vs CHX and Jo2 alone. □, CHX; ■, Jo2 + CHX; ▒, Jo2 + CHX + GLU; ▤, Jo2 + CHX + FSK.

Primary Hepatocyte Isolation, Culture, and Adenoviral Infection

Male C57BL/6 or Gcgr^{-/-} mice (8–12 weeks old) were anesthetized with isoflurane/oxygen and hepatocytes were isolated by retrograde, nonrecirculating, in situ collagenase liver perfusion. Cell viability assessed with

trypan blue was consistently greater than 90%. Hepatocytes were plated at a density of 40,000–50,000 cells/cm² and were allowed to attach for at least 3 hours before replacement of media with William’s E medium lacking serum and insulin and the indicated reagents for 4–5 hours.

RNA Preparation and Quantitative Real-Time Reverse-Transcription Polymerase Chain Reaction

Total RNA was prepared using Tri-Reagent (Sigma-Aldrich). First-strand complementary DNA was synthesized using the Superscript II synthesis system (Invitrogen) and random hexamers. Real-time polymerase chain reaction analysis was performed using TaqMan Gene Expression Assays and TaqMan Universal polymerase chain reaction master mix (Applied Biosystems, Foster City, CA) using the ABI prism 7900 Sequence Detection System (AME Bioscience, Toroeed, Norway). The primers used were Mm00433546_m1 for the mouse glucagon receptor and Hs99999901_s1 for 18S rRNA (Applied Biosystems).

Adenoviral Transduction

Adenoviruses carrying the rGcgr or LacZ gene were constructed in the laboratory of Chris Rhodes.¹² Transduction of hepatocyte cultures was performed in William’s E media without serum or insulin at a multiplicity of infection of 1500 for 12–14 hours. Media then was removed and replaced with serum-free medium containing the indicated reagents for 5–6 hours.

Sodium Dodecyl Sulfate–Polyacrylamide Gel Electrophoresis and Western Blot Analysis

After sodium dodecyl sulfate–polyacrylamide electrophoresis, proteins were electrotransferred onto a Hybond-C nitrocellulose membrane (Amersham, Piscataway, NJ). Blots were incubated with primary antibody overnight at room temperature. Proteins were detected

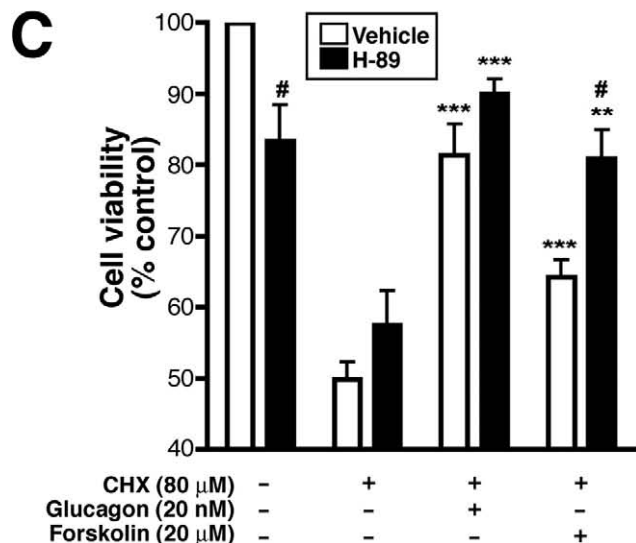
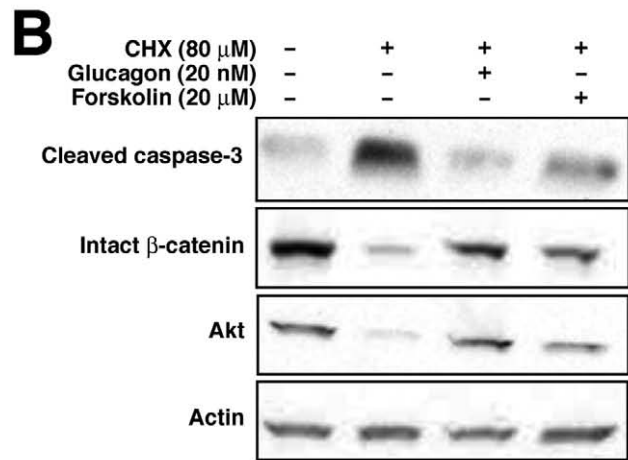
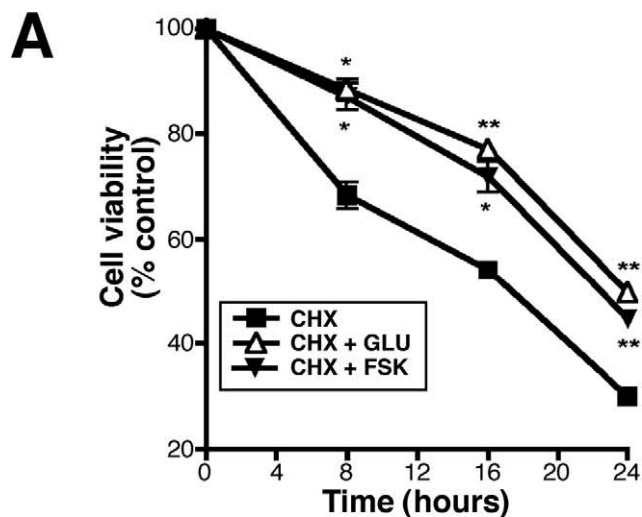


Figure 2. Glucagon and forskolin protect BHK-rGcgr cells from CHX-induced cytotoxicity. (A) Cells were treated with 80 μmol/L CHX in the presence or absence of 20 nmol/L glucagon or 20 μmol/L forskolin and cell viability was measured by a tetrazolium salt bioreduction assay and expressed as a percentage of the cell viability at time zero. Data are the means ± SEM from 4 independent experiments *P < .05, **P < .01, CHX vs CHX plus glucagon or forskolin. ■, CHX; Δ, CHX + GLU; ▼, CHX + FSK. (B) Cultures were treated with vehicle alone or with 80 μmol/L CHX with or without 20 nmol/L glucagon or 20 μmol/L forskolin for 16 hours. Whole cell extracts were analyzed by immunoblotting for cleaved caspase-3, intact β-catenin, and total Akt. (C) Cells were treated with 10 μmol/L H-89 (■) or vehicle (□) 30 minutes before and during a 16-hour incubation with 80 μmol/L CHX with or without 20 nmol/L glucagon or 20 μmol/L forskolin. Cell viability was determined as in A. Data are the means ± SD of 4 independent experiments. **P < .01, ***P < .001, CHX plus glucagon or forskolin vs CHX alone; #P < .05 vehicle vs H-89.

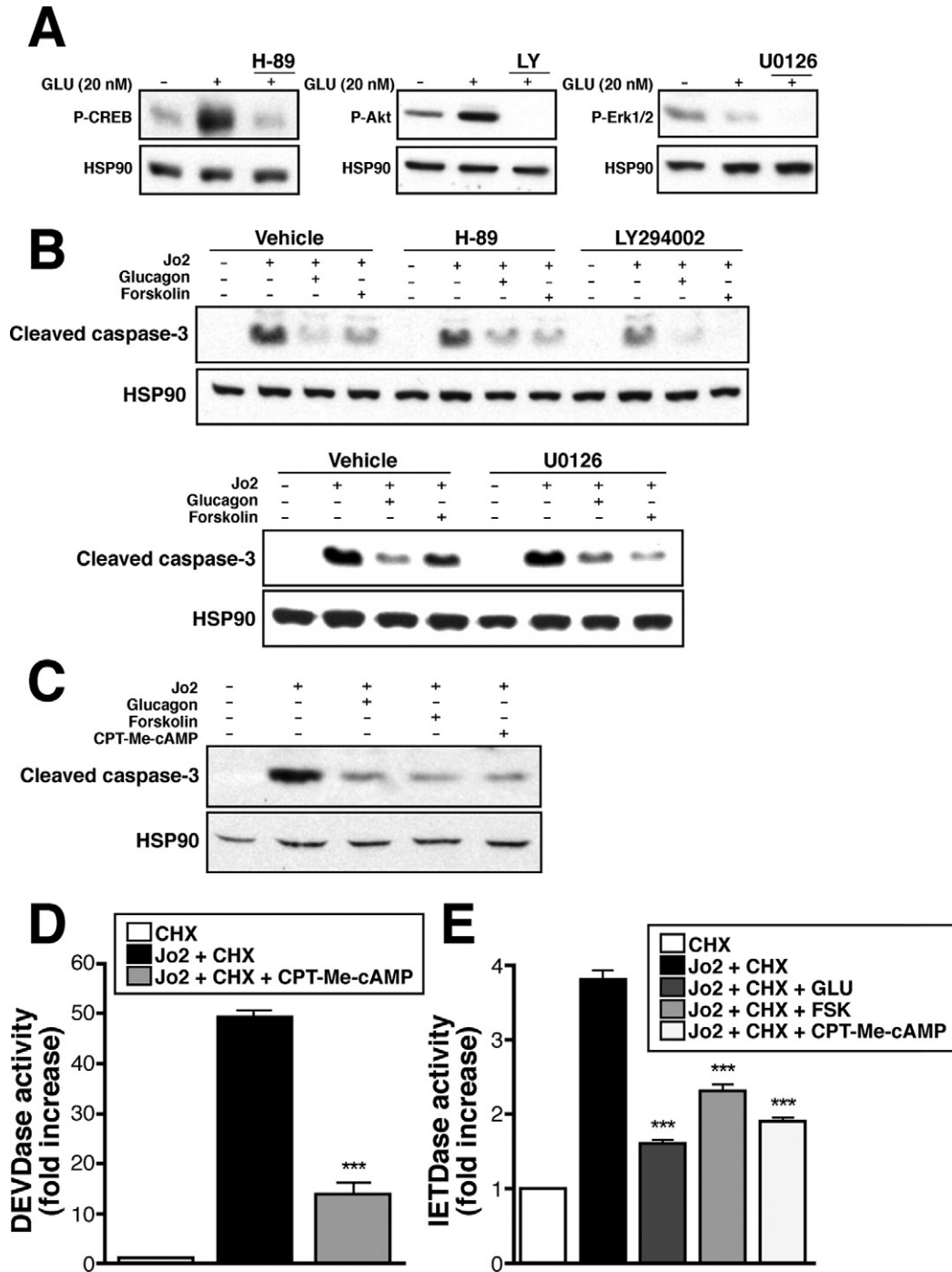
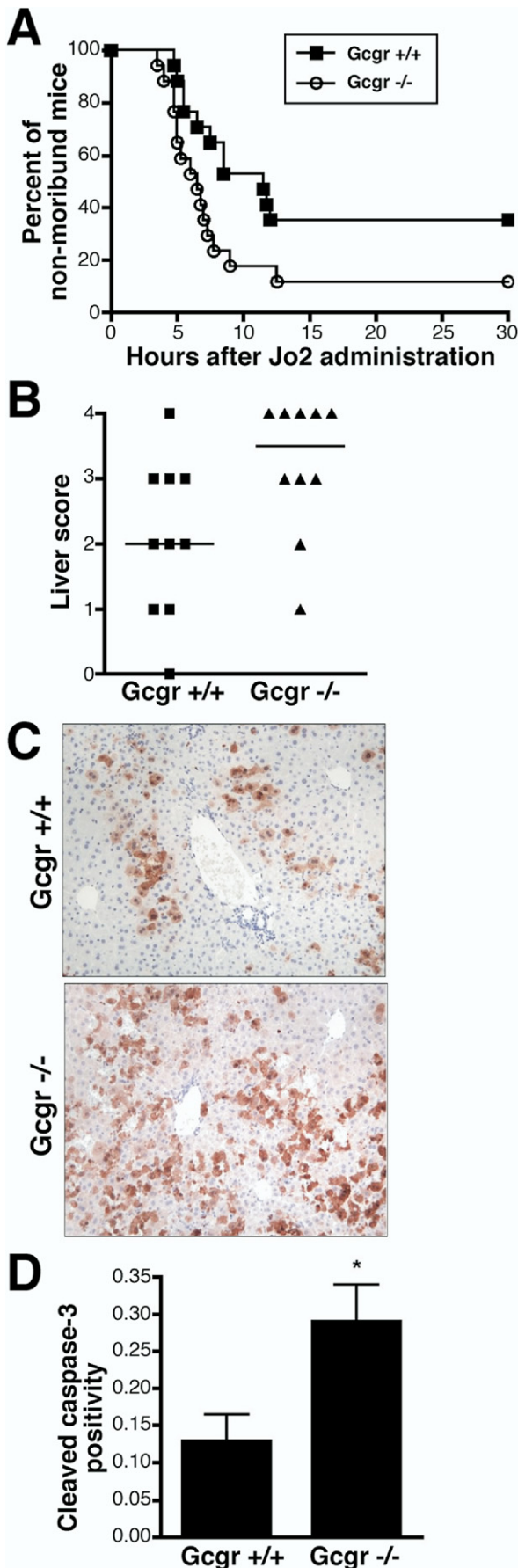


Figure 3. Glucagon, forskolin, and the Epac agonist CPT-Me-cAMP protect primary mouse hepatocytes from Jo2-induced apoptosis. (A) Hepatocyte cultures were serum-starved for 4–5 hours before pre-incubating with 10 $\mu\text{mol/L}$ H-89, 50 $\mu\text{mol/L}$ LY294002, 20 $\mu\text{mol/L}$ U0126, or vehicle alone for 30 minutes. Cells then were stimulated for 10 minutes with either vehicle or 20 nmol/L glucagon, whereupon cell extracts were analyzed by immunoblotting with phospho-specific antibodies for CREB (H-89–treated cultures), Akt (LY294002-treated cultures), and Erk1/2 mitogen-activated protein kinase (U0126-treated cultures). Results are representative of 2–3 independent experiments. (B and C) Hepatocytes were pre-incubated with protein kinase inhibitors for 30 minutes before and during a 4- to 5-hour treatment with 10 $\mu\text{mol/L}$ CHX or 10 $\mu\text{mol/L}$ CHX plus 100 ng/mL Jo2 with or without 2 nmol/L glucagon or 20 $\mu\text{mol/L}$ forskolin. Apoptosis was quantified by immunoblotting for cleaved caspase-3. (D) DEVDase and (E) IETDase enzymatic activity was assessed in hepatocytes treated for 4–5 hours with 10 $\mu\text{mol/L}$ CHX or 10 $\mu\text{mol/L}$ CHX plus 100 ng/mL Jo2 alone or with $\mu\text{mol/L}$ CPT-Me-cAMP or (E) glucagon or forskolin. Data are means \pm SD and are representative of 2–3 independent experiments performed in duplicate. *** $P < .001$, CHX plus Jo2 vs CHX plus Jo2 plus either glucagon, forskolin, or CPT-Me-cAMP. (D) \square , CH; \blacksquare , Jo2 + CHX; \square , Jo2 + CHX + CPT-Me-cAMP. (E) \square , CH; \blacksquare , Jo2 + CHX; \blacksquare , Jo2 + CHX + GLU; \blacksquare , Jo2 + CHX + FSK; \square , Jo2 + CHX + CPT-Me-cAMP.



with a second antibody conjugated to horseradish peroxidase and an enhanced chemiluminescence kit (Amersham). Primary antibodies were used at the following dilutions: cleaved caspase-3, total Akt, phospho-Akt (Ser 473), Bcl-2, Bcl-xl, phospho-CREB (Ser 133), phospho-p44/42 mitogen-activated protein kinase (Thr202/Tyr204) (Cell Signaling, Danvers, MA) 1:1000; actin (Sigma-Aldrich) 1:5000; β -catenin 1:500; HSP90 (BD Biosciences) 1:2000; and Bcl-2 interacting domain (R&D Systems, Minneapolis, MN) 1:1000.

Quantification of Apoptosis in Mouse Hepatocyte Cultures

Apoptosis was assessed using the Cell Death Detection enzyme-linked immunosorbent assay^{PLUS} (Roche) through determination of cytoplasmic histone-associated DNA fragments (mononucleosomes and oligonucleosomes). Alternatively, cells were fixed in 4% paraformaldehyde, nuclei were stained with 20 ng/mL 4'-6-diamidino-2-phenylindole in phosphate-buffered saline (PBS), and scored as apoptotic or healthy according to morphologic criteria.¹³ A minimum of 100 nuclei was counted from 4 fields within each treatment. Images were recorded using a Leica DM 1RB microscope, DC 300F camera, and Leica IM5000 software (version 1.2; Leica Microsystems, Bannockburn, IL).

Caspase Activity Assay

Caspase enzymatic activity was assessed by cleavage of fluorogenic substrates (7-amino-4-methylcoumarin) with the specificity of Ile-Glu-Thr-Asp (caspase-8 and -10) or Asp-Glu-Val-Asp (caspase-3 and -7) (Biomol International, Plymouth Meeting, PA). Hepatocytes were lysed at 4°C in 50 mmol/L HEPES, pH 7.4, 75 mmol/L NaCl, 1% Triton X-100, 1 mmol/L ethylenediaminetetraacetic acid, 1 mmol/L dithiothreitol, 1 mmol/L phenylmethylsulfonyl fluoride, 10 μ g/mL pepstatin A, and 100 KIU/mL aprotinin (Trasylol; Bayer, Pittsburgh, PA), centrifuged at 4°C, and the supernatant was recovered. Enzymatic assays were performed at room temperature, using 50 μ g of cell lysate and 100 μ mol/L of fluorogenic substrate in 100 mmol/L HEPES, pH 7.4, 150 mmol/L NaCl, 0.2% CHAPS, 20 mmol/L dithiothreitol, and 20%

Figure 4. Gcgr^{-/-} mice show enhanced susceptibility to Jo2-induced liver apoptosis. (A) Gcgr^{-/-} (○) and Gcgr^{+/+} (■) male mice were injected with 10 μ g Jo2 intraperitoneally and monitored closely for signs of clinical compromise whereupon they were euthanized. **P* < .05, Gcgr^{-/-} vs Gcgr^{+/+}, n = 17 per group. (B-D) Mice were injected intraperitoneally with 10 μ g Jo2 for 4 hours whereupon liver tissue samples were taken for analysis, n = 10 per genotype. (B) Individual hepatic apoptosis scores were assessed after H&E staining of liver tissue sections. The horizontal line indicates the median. (C) Immunohistochemical detection of cleaved caspase-3 in liver sections from mice after Jo2 challenge (magnification, 100 \times). (D) Quantification of cleaved caspase-3 staining from liver sections of Gcgr^{+/+} and Gcgr^{-/-} mice.

glycerol. Caspase-catalyzed release of the fluorophore 7-amino-4-methylcoumarin was monitored by fluorometric analysis (SpectraMax, Gemini; Molecular Devices Corp, Sunnyvale, CA) with an excitation of 380 nm and emission at 460 nm.

Animal Experiments

All animal experiments were approved by the Toronto General Hospital Animal Care Committee. Male *Gcgr*^{-/-} mice, 8–12 weeks of age² in the C57BL/6 background and littermate controls (*Gcgr*^{+/+}) were assessed for susceptibility to hepatocyte apoptosis using 10 μg of Jo2 administered by intraperitoneal injection. Mice were euthanized either after 4 hours or if they showed signs of clinical compromise according to Animal Care

Guidelines. For analysis of glucagon action in vivo, C57BL/6 male mice (8–9 weeks old) were purchased from Charles River Laboratories (Wilmington, MA), allowed to acclimatize for 1 week, then injected subcutaneously with either 30 ng/g/body weight glucagon in 10% gelatin or gelatin alone. After 30 minutes mice were injected with either 20 μg Jo2 or PBS and euthanized after 6 hours. For experiments using specific diets, male mice were fed a diet either deficient in methionine and choline (A02082002B) or a control diet (A02082003B) from Research Diets Inc (New Brunswick, NJ). For adenoviral (Ad) transduction in mice, adenovirus (1 × 10⁹ plaque-forming units) encoding the r*Gcgr* or LacZ genes was administered by tail vein injection to 8- to 12-week-old *Gcgr*^{-/-} mice. Five days later mice were treated with either 10 μg of Jo2 or PBS and euthanized after 4 hours.

Liver Histology

Histopathologic evaluation of liver sections for quantification of apoptosis was performed as described¹⁴ in a blinded manner using the following scoring system: 0, normal (no apoptosis); 1, minimal apoptosis (rare/occasional apoptotic bodies <5%); 2, mild apoptosis (up to 25% positivity); 3, moderate apoptosis (up to 75% positivity); and 4, severe apoptosis (75%–100% positivity). For lipid oil red O staining, hepatic steatosis was scored as follows: 0, 0%; 1, 0%–33%; 2, 33%–67%; and 3, 67%–100%. Quantification of cleaved caspase-3 and steatosis in liver sections was performed using the Scanscope slide scanning system and Aperio Positive Pixel Count Algorithm (Aperio Technologies, Inc, Vista, CA).

Statistical Analysis

The statistical significance of differences between *Gcgr*^{+/+} and *Gcgr*^{-/-} mice administered Jo2 was an-

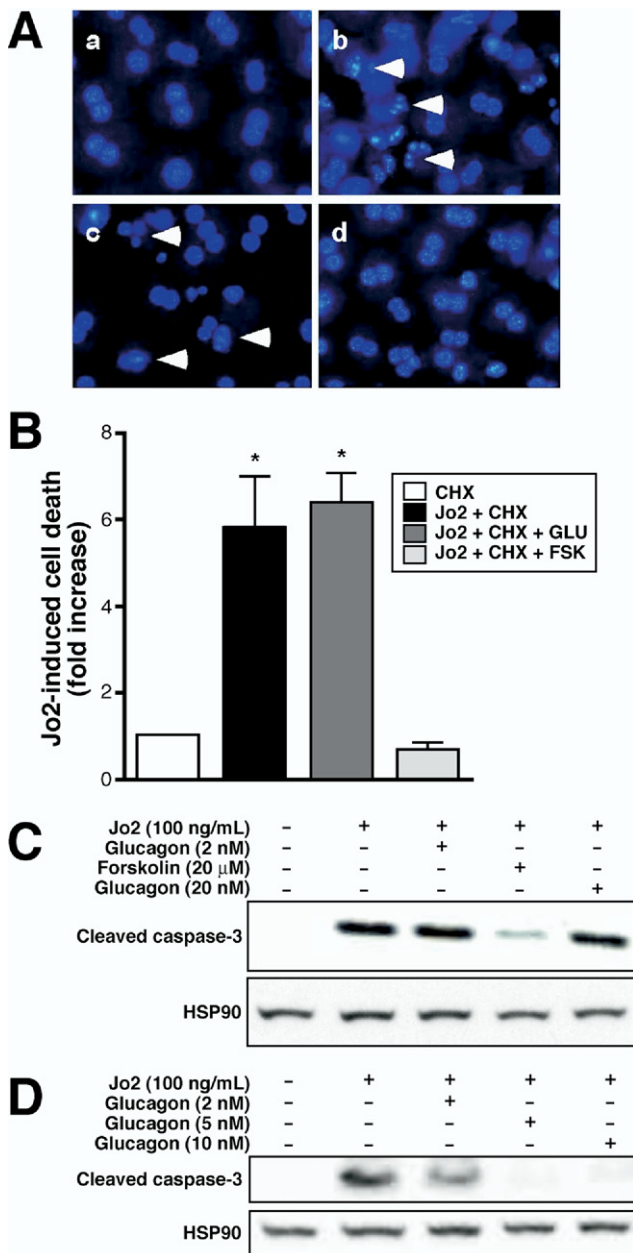


Figure 5. Expression of r*Gcgr* in *Gcgr*^{-/-} hepatocytes restores the cytoprotective effect of glucagon. (A) Primary hepatocytes from *Gcgr*^{-/-} mice were incubated for 4–5 hours with 10 μmol/L CHX (a), 10 μmol/L CHX plus 100 ng/mL Jo2, in the absence (b) or presence of 2 nmol/L glucagon (c) or 20 μmol/L forskolin (d), and stained with 4'-6-diamidino-2-phenylindole. Arrowheads indicate cells undergoing apoptosis. (B) Apoptosis was quantified by Cell Death enzyme-linked immunosorbent assay in cells treated for 4–5 hours as indicated in A, except that the glucagon concentration was 20 nmol/L. Data are mean ± SD and are representative of 2 independent experiments performed in duplicate, **P* < .05, CHX-alone vs CHX plus Jo2 in the presence or absence of glucagon or forskolin. □, CHX; ■, Jo2 + CHX; ▒, Jo2 + CHX + GLU; ▤, Jo2 + CHX + FSK. (C) Western blot analysis of cell extracts from *Gcgr*^{-/-} hepatocytes treated with 10 μmol/L CHX or 10 μmol/L CHX plus Jo2 in the absence or presence of either glucagon or forskolin as indicated. Blots are representative of 3 independent experiments. (D) Isolated *Gcgr*^{-/-} mouse hepatocytes were transduced with a r*Gcgr* adenovirus (multiplicity of infection, 1500) for 12–14 hours in serum-free conditions. Cells then were treated with 10 μmol/L CHX and Jo2 in the absence or presence of glucagon. Cell extracts were prepared after 5–6 hours for immunoblot analysis. Blots are representative of 2 independent experiments.

alyzed by log-rank or by Mann–Whitney tests. Otherwise, data were analyzed by *t* test or using analysis of variance where appropriate, with group comparisons performed using Bonferroni multiple comparison post-test.

Results

Mouse hepatocytes showed a dose-dependent increase in levels of cAMP in response to glucagon with a half maximal effective concentration (EC_{50}) of between 0.13 and 0.8 nmol/L (supplementary Figure 1; see supplementary material online at www.gastrojournal.org). Activation of the Fas pathway with the Jo2 antibody

produced characteristic morphologic signs of apoptosis, including blebbing, chromatin condensation, and cell lysis¹³ (Figure 1A, panel b); the morphologic features of apoptosis were markedly attenuated after treatment with 2 nmol/L glucagon or 20 μ mol/L forskolin (Figure 1A, panels c and d, respectively). Similarly, glucagon significantly reduced (5- to 7-fold) the abundance of cytoplasmic mononucleosomes and oligonucleosomes (Figure 1B) and both glucagon and forskolin markedly reduced levels of cleaved caspase-3 (Figure 1C) and caspase-3-like DEVD hydrolase activity after Jo2-induced apoptosis (Figure 1D). Glucagon also reduced hepatocyte apoptosis after

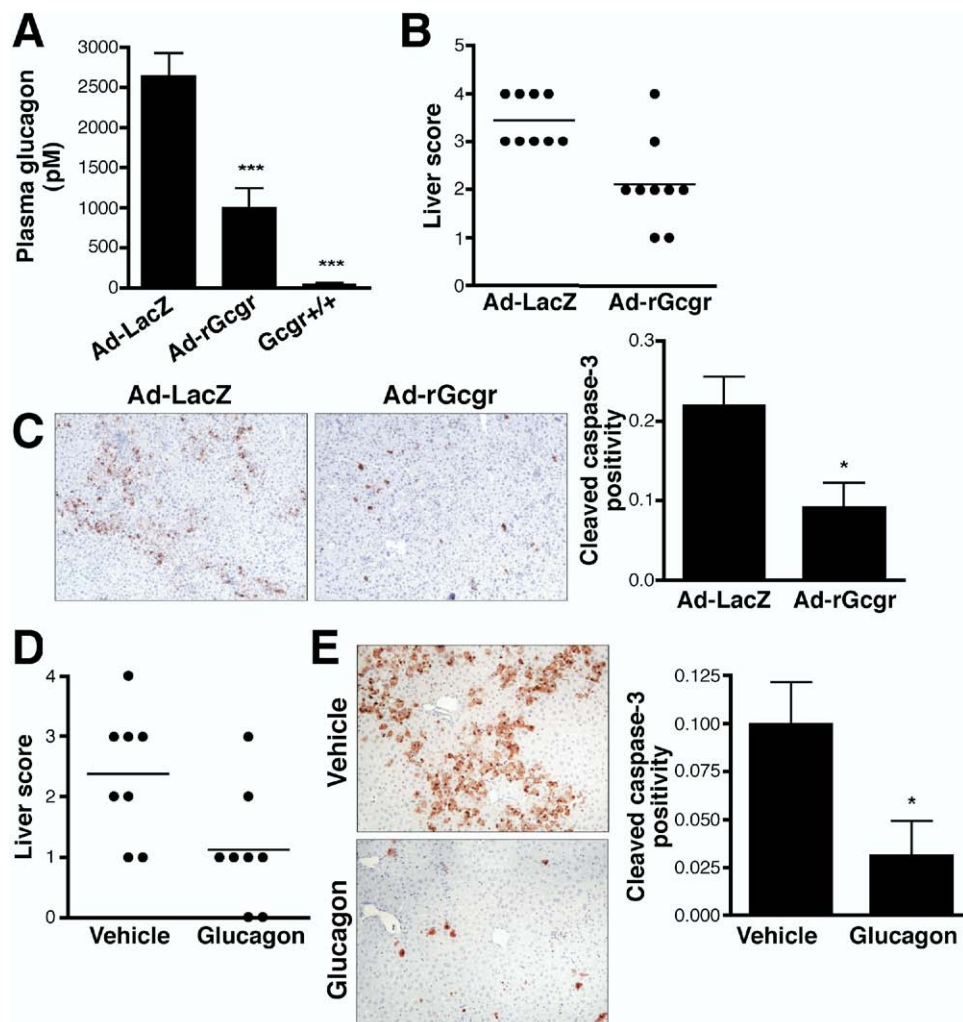


Figure 6. Adenoviral rescue of the glucagon receptor in *Gcgr*^{-/-} mice and exogenous glucagon administration in wild-type mice attenuates Jo2-induced apoptosis. (A) Fed-state levels of plasma glucagon in *Gcgr*^{-/-} mice 5 days after intravenous administration of 1×10^9 plaque-forming units of either Ad-LacZ, or Ad-rGcgr; glucagon levels in nontransduced *Gcgr*^{+/+} mice also are shown. Data are mean \pm SEM, $n = 6-8$, *** $P < .001$, Ad-LacZ vs Ad-Gcgr-transduced *Gcgr*^{-/-} mice or *Gcgr*^{+/+} mice. (B–C) Five days after administration of adenovirus as indicated in A, *Gcgr*^{-/-} mice were injected with 10 μ g Jo2 ($n = 9$ mice per group). After 4 hours liver samples were taken for analysis. (B) Individual hepatic apoptosis scores were assessed as per criteria stated in the Materials and Methods section. The horizontal line indicates the median. (C) Immunohistochemical and quantitative detection of cleaved caspase-3 in liver sections from either Ad-LacZ- or Ad-rGcgr-infected *Gcgr*^{-/-} mice after Jo2 administration (magnification, 50 \times). (D) Wild-type male mice were injected subcutaneously with 30 ng/g body weight of glucagon or vehicle 30 minutes before intraperitoneal injection of 20 μ g Jo2 ($n = 8$ mice per group). After 6 hours liver samples were taken for analysis. Individual hepatic apoptosis scores were assessed after H&E staining of liver tissue sections. The horizontal line indicates the median. (E) Immunohistochemical and quantitative detection of cleaved caspase-3 in liver sections from vehicle or glucagon-treated C57BL/6 mice (magnification, 100 \times). For C and E, * $P < .05$.

exposure to tumor necrosis factor- α plus actinomycin D (supplementary Figure 2; see supplementary material online at www.gastrojournal.org).

The anti-apoptotic actions of Gcgr signaling also were detected in BHK fibroblasts transfected with the rat glucagon receptor (BHK:rGcgr), which showed a dose-dependent increase of cAMP accumulation in response to glucagon (supplementary Figure 3A; see supplementary material online at www.gastrojournal.org). Cycloheximide (CHX) reduced BHK cell viability; however, 20 nmol/L glucagon or 20 μ mol/L forskolin increased cell viability in CHX-treated cells (Figure 2A). Furthermore, both glucagon and forskolin reduced levels of cleaved caspase-3, and attenuated reductions in levels of the executioner caspase substrates β -catenin and Akt (Figure 2B). The preservation of cell viability was not attributable to increased cell proliferation (supplementary Figure 3B; see supplementary material online at www.gastrojournal.org). Although both glucagon and forskolin stimulate cAMP accumulation and activate protein kinase A (PKA),¹ the PKA inhibitor H-89 did not diminish the cytoprotective actions of glucagon or forskolin in BHK:rGcgr cells (Figure 2C). Hence, the Gcgr engages anti-apoptotic signaling pathways in a PKA-independent manner.

We next examined glucagon action in murine hepatocytes. Glucagon stimulated the phosphorylation of CREB and Akt, which was inhibited by the protein kinase inhibitors H-89 and LY294002, consistent with activation of the PKA and PI-3K pathways, respectively. In contrast, glucagon reduced mitogen-activated protein kinase phosphorylation, which was reduced further by the MEK 1/2 inhibitor U0126 (Figure 3A). Remarkably, inhibition of PKA, PI-3K, or MEK 1/2 pathways did not interfere with the ability of glucagon or forskolin to attenuate Jo2-induced caspase-3 cleavage (Figure 3B) or enhance cell survival (supplementary Figure 4A; see supplementary material online at www.gastrojournal.org). Furthermore, the ability of glucagon and forskolin to phosphorylate Akt and CREB was preserved in the presence of Jo2 (supplementary Figure 4B; see supplementary material online at www.gastrojournal.org).

Because glucagon enhances cAMP formation yet exerts cytoprotective effects in a PKA-independent manner, we hypothesized that glucagon regulates apoptosis through activation of Epac, a family of cAMP-regulated guanine nucleotide exchange factors that act independently of PKA.¹⁵ Consistent with this possibility, the Epac agonist CPT-Me-cAMP mimicked the effects of glucagon, leading to reduced caspase-3 cleavage (Figure 3C) and significantly ($P < .001$) decreased caspase-3-like DEVD hydrolyase activity (Figure 3D) in mouse hepatocytes after Jo2-induced apoptosis.

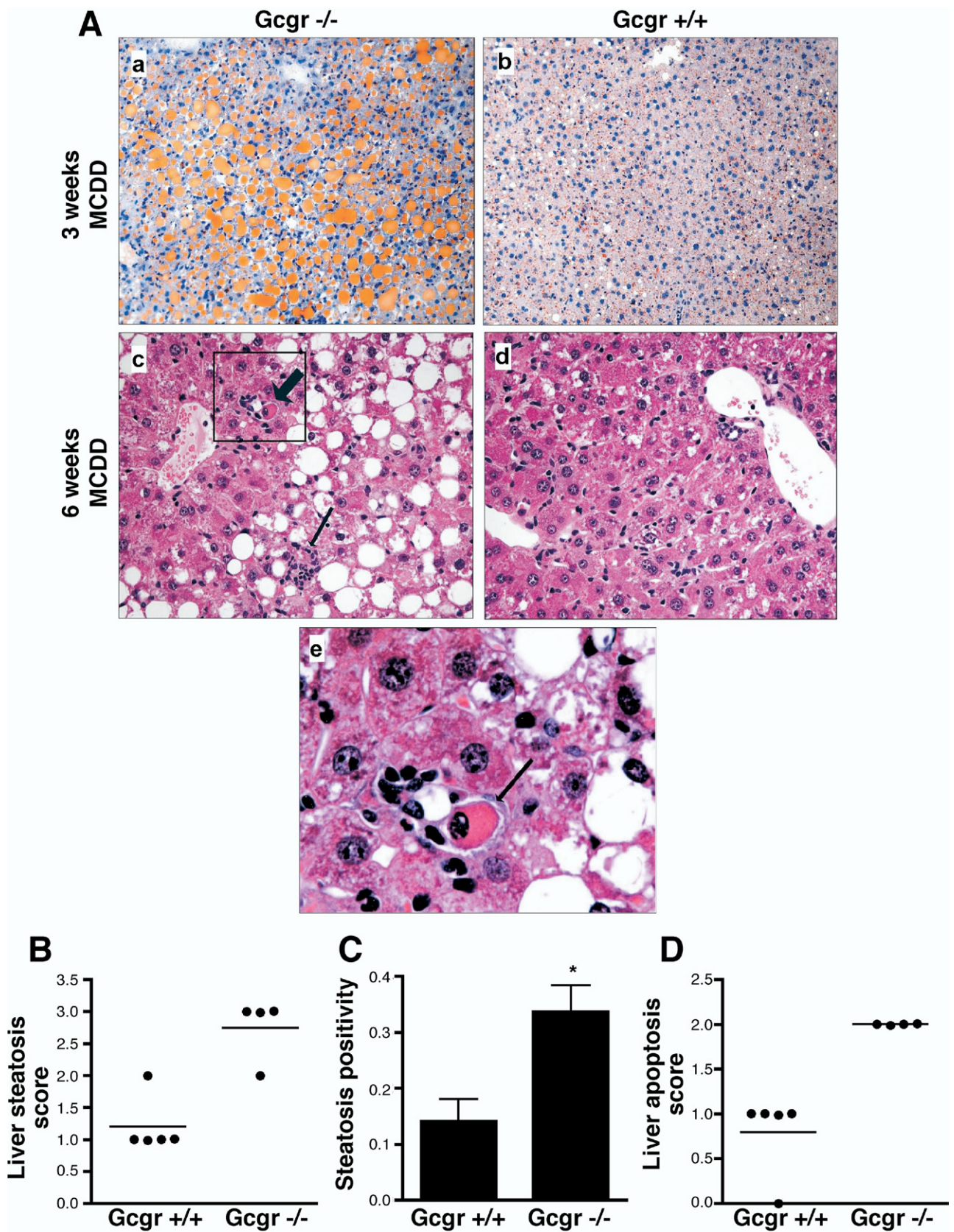
Activation of the Fas receptor leads to recruitment of an adaptor molecule Fas-associated protein with death domain that aids in Fas receptor activation and recruits and binds caspase-8, forming the death-inducing signaling complex

(DISC).¹⁶ Because cAMP may inhibit DISC formation¹⁷ we assessed whether glucagon interferes with the ability of the DISC to promote caspase-8 activation. Caspase-8 activity was increased in hepatocytes treated with Jo2 and CHX, however, co-incubation with glucagon, forskolin, or CPT-Me-cAMP attenuated caspase-8 activation (Figure 3E). In contrast, glucagon had no effect on levels of the anti-apoptotic effectors Bcl-xl or Bcl-2 (supplementary Figure 4C; see supplementary material online at www.gastrojournal.org). Hence glucagon, likely acting via cAMP and Epac, interferes with Fas-induced apoptosis at a proximal level in Fas-DISC signaling.

To determine the importance of endogenous Gcgr signaling for hepatocyte survival we assessed susceptibility to Jo2-induced liver injury in Gcgr $^{-/-}$ mice. Jo2 produced more rapid morbidity and increased mortality in Gcgr $^{-/-}$ compared with Gcgr $^{+/+}$ mice ($P < .05$; Figure 4A). Furthermore, Gcgr $^{-/-}$ mice showed a significantly greater median liver apoptotic score (Figure 4B, $P < .05$). A greater proportion of Gcgr $^{-/-}$ mice had increased serum levels of transaminases, enzymes released after liver injury, compared with Gcgr $^{+/+}$, with 64% of Gcgr $^{-/-}$ vs 33% of Gcgr $^{+/+}$ mice showing aspartate aminotransferase (AST) levels greater than 600 U/L. Similarly, 73% of Gcgr $^{-/-}$ vs 44% of Gcgr $^{+/+}$ mice had alanine aminotransferase (ALT) levels greater than 100 U/L. Immunohistochemical analyses showed more extensive cleaved caspase-3 immunopositivity in Gcgr $^{-/-}$ hepatocytes after Jo2 treatment (Figure 4C and D). These findings indicate that Gcgr $^{-/-}$ mice show enhanced susceptibility to Jo2-induced liver injury.

To address whether the enhanced sensitivity of Gcgr $^{-/-}$ mice to liver injury reflects a direct role for the Gcgr in engagement of cell survival pathways, we re-introduced the Gcgr by viral transduction into Gcgr $^{-/-}$ hepatocytes. Gcgr $^{-/-}$ hepatocytes showed no cAMP accumulation in response to glucagon, but retained responsiveness to forskolin (supplementary Figure 5A; see supplementary material online at www.gastrojournal.org). Despite increased basal levels of cAMP,² Gcgr $^{-/-}$ hepatocytes were equally susceptible to Jo2-induced apoptosis (35%–50% of both Gcgr $^{+/+}$ and Gcgr $^{-/-}$ hepatocytes showed morphologic features of apoptosis) and forskolin, but not glucagon, attenuated features of apoptosis in Gcgr $^{-/-}$ hepatocytes (Figure 5A, panels a–d). Furthermore, forskolin, but not glucagon, significantly reduced the abundance of cytoplasmic mononucleosomes and oligonucleosomes and decreased levels of cleaved caspase-3 in Jo2-treated Gcgr $^{-/-}$ hepatocytes (Figure 5B and C). Adenoviral transduction of rGcgr restored glucagon-responsive cAMP production ($EC_{50} = 0.19$ nmol/L) and the anti-apoptotic actions of glucagon in Gcgr $^{-/-}$ hepatocytes (supplementary Figure 5B and Figure 5D).

To ascertain whether partial restoration of hepatic Gcgr expression would mitigate the extent of experimental hepatic injury in vivo, we administered Ad-rGcgr to



Gcgr^{-/-} mice via intravenous infusion. Hepatic Gcgr expression in Gcgr^{-/-} mice (supplementary Figure 6A; see supplementary material online at www.gastrojournal.org) was associated with a significant reduction in plasma glucagon levels and a significant increase in ambient plasma glucose compared with Ad-LacZ-transduced mice ($P < .001$, Figure 6A; and $P < .01$, supplementary Figure 6B, respectively). Furthermore, Gcgr^{-/-} mice transduced with the Ad-rGcgr showed significantly reduced hepatic injury after Jo2 administration in vivo ($P < .01$) (Figure 6B). Moreover, a significant reduction in the number of hepatocytes showing immunopositivity for cleaved caspase-3 after Jo2 administration was observed in Ad-rGcgr vs Ad-LacZ-transduced Gcgr^{-/-} mice (Figure 6C). Exogenous glucagon also increased hepatocyte survival after liver injury in wild-type mice. Glucagon administration significantly ($P < .05$) lowered the median hepatic apoptosis score (Figure 6D) and fewer glucagon-treated mice showed increased levels (>300 U/L) of serum AST (12.5% vs 50%) and ALT (25% vs 50%) compared with vehicle-treated mice. Furthermore, glucagon markedly reduced the extent of cleaved caspase-3 immunopositivity in liver (Figure 6E; $P < .05$).

We next examined the susceptibility of Gcgr^{-/-} mice to diet-induced liver injury. Gcgr^{+/+} and Gcgr^{-/-} mice were fed a methionine and choline-deficient diet known to produce experimental liver injury with histopathologic abnormalities characteristic of nonalcoholic steatohepatitis.¹⁸ Control Gcgr^{+/+} and Gcgr^{-/-} mice received the identical diet supplemented with methionine and choline. Histologic examination of liver tissue showed a significantly greater accumulation of lipid in Gcgr^{-/-} mice (Figure 7A, panel a and b and Figure 7B and C; $P < .05$) despite similar levels of food intake, and comparable changes in body weight in both groups of mice (supplementary Figure 7A and B; see supplementary material online at www.gastrojournal.org). Consistent with the greater degree of liver injury (Figure 7A, panels c-e), plasma glucose was lower in Gcgr^{-/-} mice (supplementary Figure 7C; see supplementary material online at www.gastrojournal.org). Furthermore, histologic features of apoptosis were more evident in Gcgr^{-/-} mice after 6 weeks on the methionine and choline-deficient diet (Figure 7A, panel c and d, quantified in Figure 7D; $P < .05$). Taken together, these findings show that loss of Gcgr signaling increases hepatocyte susceptibility to liver injury.

Discussion

Signaling through class B G-protein-coupled receptors⁸ is known to promote cell survival. For example, GLP-2

directly reduces apoptosis in cells¹⁹ and in rodents with experimental intestinal injury.²⁰ Similarly, GLP-1-receptor activation reduced cell death in rodent insulinomas and in rodent and human pancreatic islet β -cells.²¹ Conversely, Glp1r^{-/-} β cells display enhanced susceptibility to apoptotic injury.²² Our observations extend these concepts by establishing that endogenous Gcgr signaling plays an essential role in the control of hepatocyte survival.

A potential pathway linking proglucagon-derived peptide receptor activation to control of cell survival is via cAMP²³ because cAMP levels influence cell survival in diverse cell types including hepatocytes.^{10,24,25} The observation that glucagon, CPT-Me-cAMP, and forskolin enhance cell survival in murine hepatocytes is consistent with accumulating evidence invoking a critical role for cAMP as a key determinant of hepatocyte viability. Although activation of PKA, PI-3K, and Erk1/2 mitogen-activated protein kinase pathways has been linked to enhanced hepatocyte survival,²⁵⁻²⁸ the effects of glucagon to reduce Jo2-induced hepatocyte apoptosis were independent of these signaling pathways. Accordingly, our data are consistent with a role for Epac as a potential downstream mediator of cAMP-dependent, PKA-independent regulation of hepatocyte survival.²⁴

Several studies have identified a role for cAMP in modulating Fas Ligand (FasL)/CD95 signaling in hepatocytes, resulting in the attenuation of cell death.^{10,17} After FasL binding to CD95, the adaptor molecule Fas-associated protein with death domain is recruited and activates the Fas receptor, leading to subsequent recruitment of caspase-8 to form the DISC.¹⁶ The assembly of the DISC is critical for further downstream apoptotic signaling. Our experiments provide mechanistic understanding of how the Gcgr enhances hepatocyte viability by showing that glucagon and the Epac agonist (CPT-Me-cAMP) inhibit caspase-3 and caspase-8 activity in injured hepatocytes. These findings suggest that attenuation of Fas-induced apoptosis by glucagon and the Epac agonist likely occurs at the level of the formation of the DISC.

Our data showing that Gcgr^{-/-} mice show enhanced susceptibility to diet-induced liver injury is consistent with observations linking diet-induced hepatic steatosis with reduced Gcgr expression and decreased sensitivity to glucagon in vivo. Moreover, glucagon directly reduces hepatocyte and fibroblast apoptosis in vitro, strongly implicating the Gcgr as a direct modulator of apoptosis. The demonstration that Gcgr^{-/-} mice are more sensitive to the development of steatohepatitis and FasL-induced hepatocyte apoptosis may have implications for

Figure 7. Gcgr^{-/-} mice are more susceptible to the development of steatohepatitis. (A) Oil red O (a and b, magnification, 100 \times) and H&E (c and d, magnification, 200 \times) staining of liver from Gcgr^{-/-} (a and c) and Gcgr^{+/+} (b and d) mice after 3 weeks (oil red O staining) or 6 weeks (H&E) on a methionine and choline-deficient diet (MCD). The *thick arrow* in panel c identifies an apoptotic cell and the *thin arrow* designates an area of inflammation with an apoptotic cell in the center. A higher-power image of the apoptotic cell in panel c is shown in panel e. (B) Individual hepatic steatosis score, (C) quantification of steatosis, and (D) individual hepatic apoptosis scores in Gcgr^{-/-} and Gcgr^{+/+} mice after 6 weeks on the MCD diet. The *horizontal line* in B and D indicates the median. * $P < .05$.

strategies directed at interruption of glucagon action for the treatment of type 2 diabetes.^{2,3,6,7,29} The improvement in glucose control mediated by reduced glucagon action theoretically may be accompanied, in vulnerable diabetic subjects, by an increased susceptibility to liver injury. Our studies imply that a threshold level of hepatocyte Gcgr signaling may be optimal for hepatocellular survival. Hence, a more detailed understanding of the relationship between Gcgr signaling and hepatocyte survival under diverse metabolic circumstances seems warranted.

Supplementary Data

Note: To access the supplementary material accompanying this article, visit the online version of *Gastroenterology* at www.gastrojournal.org, and at doi: [10.1053/j.gastro.2008.07.075](https://doi.org/10.1053/j.gastro.2008.07.075).

References

- Jiang G, Zhang BB. Glucagon and regulation of glucose metabolism. *Am J Physiol Endocrinol Metab* 2003;284:E671–E678.
- Gelling RW, Du XQ, Dichmann DS, et al. Lower blood glucose, hyperglucagonemia, and pancreatic {alpha} cell hyperplasia in glucagon receptor knockout mice. *Proc Natl Acad Sci U S A* 2003;100:1438–1443.
- Sorensen H, Winzell MS, Brand CL, et al. Glucagon receptor knockout mice display increased insulin sensitivity and impaired {beta}-cell function. *Diabetes* 2006;55:3463–3469.
- Conarello SL, Jiang G, Mu J, et al. Glucagon receptor knockout mice are resistant to diet-induced obesity and streptozotocin-mediated beta cell loss and hyperglycaemia. *Diabetologia* 2007; 50:142–150.
- Riddle MC, Drucker DJ. Emerging therapies mimicking the effects of amylin and glucagon-like peptide 1. *Diabetes Care* 2006;29:435–449.
- Liang Y, Osborne MC, Monia BP, et al. Reduction in glucagon receptor expression by an antisense oligonucleotide ameliorates diabetic syndrome in db/db mice. *Diabetes* 2004;53:410–417.
- Sloop KW, Cao JX, Siesky AM, et al. Hepatic and glucagon-like peptide-1-mediated reversal of diabetes by glucagon receptor antisense oligonucleotide inhibitors. *J Clin Invest* 2004;113: 1571–1581.
- Mayo KE, Miller LJ, Bataille D, et al. International Union of Pharmacology. XXXV. The Glucagon Receptor Family. *Pharmacol Rev* 2003;55:167–194.
- Armato U, Romano F, Andreis PG, et al. Growth stimulation and apoptosis induced in cultures of neonatal rat liver cells by repeated exposures to epidermal growth factor/urogastrone with or without associated pancreatic hormones. *Cell Tissue Res* 1986; 245:471–480.
- Fladmark KE, Gjertsen BT, Doskeland SO, et al. Fas/APO-1(CD95)-induced apoptosis of primary hepatocytes is inhibited by cAMP. *Biochem Biophys Res Commun* 1997;232:20–25.
- Baggio LL, Huang Q, Brown TJ, et al. Oxyntomodulin and glucagon-like peptide-1 differentially regulate murine food intake and energy expenditure. *Gastroenterology* 2004;127:546–558.
- Dickson LM, Lingohr MK, McCuaig J, et al. Differential activation of protein kinase B and p70(S6)K by glucose and insulin-like growth factor 1 in pancreatic beta-cells (INS-1). *J Biol Chem* 2001;276:21110–21120.
- Lawen A. Apoptosis—an introduction. *Bioessays* 2003;25:888–896.
- Scheuer PJ. Classification of chronic viral hepatitis: a need for reassessment. *J Hepatol* 1991;13:372–374.
- Holz GG. Epac: a new cAMP-binding protein in support of glucagon-like peptide-1 receptor-mediated signal transduction in the pancreatic beta-cell. *Diabetes* 2004;53:5–13.
- Nagata S. Fas ligand-induced apoptosis. *Annu Rev Genet* 1999; 33:29–55.
- Reinehr R, Haussinger D. Inhibition of bile salt-induced apoptosis by cyclic AMP involves serine/threonine phosphorylation of CD95. *Gastroenterology* 2004;126:249–262.
- Koteish A, Mae Diehl A. Animal models of steatohepatitis. *Best Pract Res Clin Gastroenterol* 2002;16:679–690.
- Yusta B, Boushey RP, Drucker DJ. The glucagon-like peptide-2 receptor mediates direct inhibition of cellular apoptosis via a cAMP-dependent protein kinase-independent pathway. *J Biol Chem* 2000;275:35345–35352.
- Boushey RP, Yusta B, Drucker DJ. Glucagon-like peptide 2 decreases mortality and reduces the severity of indomethacin-induced murine enteritis. *Am J Physiol* 1999;277:E937–E947.
- Brubaker PL, Drucker DJ. Glucagon-like peptides regulate cell proliferation and apoptosis in the pancreas, gut and central nervous system. *Endocrinology* 2004;145:2653–2659.
- Li Y, Hansotia T, Yusta B, et al. Glucagon-like peptide-1 receptor signaling modulates beta cell apoptosis. *J Biol Chem* 2003;278: 471–478.
- Drucker DJ. Glucagon-like peptides: regulators of cell proliferation, differentiation, and apoptosis. *Mol Endocrinol* 2003;17: 161–171.
- Cullen KA, McCool J, Anwer MS, et al. Activation of cAMP-guanine exchange factor confers PKA-independent protection from hepatocyte apoptosis. *Am J Physiol Gastrointest Liver Physiol* 2004; 287:G334–G343.
- Graf D, Reinehr R, Kurz AK, et al. Inhibition of tauroolithocholate 3-sulfate-induced apoptosis by cyclic AMP in rat hepatocytes involves protein kinase A-dependent and -independent mechanisms. *Arch Biochem Biophys* 2003;415:34–42.
- Qiao L, Han SI, Fang Y, et al. Bile acid regulation of C/EBPbeta, CREB, and c-Jun function, via the extracellular signal-regulated kinase and c-Jun NH2-terminal kinase pathways, modulates the apoptotic response of hepatocytes. *Mol Cell Biol* 2003;23:3052–3066.
- Simon MT, Pauloin A, Normand G, et al. HIP/PAP stimulates liver regeneration after partial hepatectomy and combines mitogenic and anti-apoptotic functions through the PKA signaling pathway. *FASEB J* 2003;17:1441–1450.
- Rust C, Bauchmuller K, Fickert P, et al. Phosphatidylinositol 3-kinase-dependent signaling modulates taurochenodeoxycholic acid-induced liver injury and cholestasis in perfused rat livers. *Am J Physiol Gastrointest Liver Physiol* 2005;289:G88–G94.
- Qureshi SA, Rios Candelore M, Xie D, et al. A novel glucagon receptor antagonist inhibits glucagon-mediated biological effects. *Diabetes* 2004;53:3267–3273.

Received December 3, 2007. Accepted July 24, 2008.

Address reprint requests to: Daniel J. Drucker, MD, Mount Sinai Hospital, Samuel Lunenfeld Research Institute, 60 Murray Street, Mailbox 39, Toronto, Ontario M5T 3L9, Canada. e-mail: d.drucker@utoronto.ca; fax: (416) 361-2669.

The authors disclose the following: Dr Drucker consults for companies developing diabetes therapeutics as disclosed at <http://www.glucagon.com/druckerlab.html>. These studies were supported by an operating grant from the Canadian Institutes for Health Research MOP-10903, the Canada Research Chairs Program (D.J.D.), and by National Institutes of Health grant R01 DK47425 (M.C.).